ELSEVIER

Journal of Alloys and Compounds 228 (1995) 143–147

Journal of ALLOYS AND COMPOUNDS

Electronic structure of chalcogenide compounds from the system Tl_2S–Sb_2S_3 studied by XPS and XES[1]

A. Gheorghiu[a], I. Lampre[a], S. Dupont[a], C. Sénémaud[a], M.A. El Idrissi Raghni[b], P.E. Lippens[b], J. Olivier-Fourcade[b]

[a] *Laboratoire de Chimie-Physique, Matière et Rayonnement, URA CNRS 176, Université Pierre et Marie Curie, 11 rue Pierre et Marie Curie, 75231 Paris, Cédex 05, France*

[b] *Laboratoire de Physicochimie des Matériaux Solides URA CNRS 407, Université Montpellier II-Sciences Techniques du Lanquedoc, Place Eugène Bataillon, 34095 Montpellier, Cédex 05, France*

Received 23 January 1995; in final form 4 April 1995

Abstract

X-ray photoelectron (XPS) and soft X-ray emission (XES) spectroscopies have been used as complementary methods to study the electronic structure of Tl_2S, Sb_2S_3, $TlSbS_2$ and $TlSb_3S_5$. XPS provides the binding energy (BE) of core levels as well as the total valence band (VB) distributions; XES probes the S 3p VB density of states. S 2p core level study shows that the charge transfer to sulphur atoms is noticeably higher in Tl_2S than in Sb_2S_3 and ternary compounds. From a comparison of XPS and XES results, we conclude that S 3p states are located near the top of the band in all cases; the results are discussed with reference to density of state calculations.

Keywords: Chalcogenide compounds; Electronic structure; XPS; XES

1. Introduction

Recently much interest has been devoted to new non-conventional complex materials formed from chalcogenide elements (S, Se, Te) and "lone pair" elements (Sn^{II}, As^{III}, Sb^{III}, Te^{IV}). Owing to the formation of various atomic arrangements, these systems are characterized by a large range of physical properties and offer many potential applications, especially in optoelectronics [1,2]. In the case of antimony chalcogenides, the links between the atomic structure and the electronic properties have been studied from experimental investigations using a number of complementary technics: Mössbauer, X-ray diffraction, X-ray absorption spectroscopies [3–5], as well as from theoretical studies [6]. The importance of the stereochemical activity of the antimony lone pair for the understanding of the physical properties of these systems has been evidenced [6,7].

We report in this paper a study of the electronic structure of chalcogenide compounds by means of X-ray photoelectron spectroscopy (XPS) and soft X-ray emission spectroscopy (XES). Tl_2S and Sb_2S_3 binary compounds and two ternary compounds belonging to the Tl_2S–Sb_2S_3 system ($TlSbS_2$ and $TlSb_3S_5$) have been studied. By XPS we have analysed the core levels of Tl, Sb and S atoms which are sensitive to the local bonding of each atomic site, and the total valence band distribution. By XES, electronic transitions between the valence band and the S 1s core level have been studied for each compound. Because of selection rules the spectral distributions correspond to S 3p states. Owing to an energy calibration of XPS and XES spectra by reference to the Fermi level it is possible to locate the S 3p states in the valence band distribution. Our experimental results on the valence

[1] Paper presented at the "Chalcogenides 94" workshop, 26 January 1994, CNRS, France.

SSDI 0925-8388(95)01663-5

band states are discussed in relation to band structure calculations performed in the tight-binding approach.

2. Experiments

The chalcogenide samples were prepared by chemical synthesis from the elements in the case of binary compounds and from a mixture of a suitable proportion of the binary compounds in the case of ternary systems [8]. The powders obtained by crushing were deposited as a uniform layer onto metallic supports adapted to each technique (XPS and XES).

X-ray-induced photoelectron spectra were obtained with a non-monochromatized MgKα radiation (main peak $\alpha_{1,2}$ at $h\nu = 1253.6$ eV) and an electrostatic hemispherical analyser used in the fixed analyser transmission mode (FAT). The overall resolution is estimated from the width (FWHM) of the Ag $3d_{5/2}$ peak, equal to 0.8 eV. Except for Tl_2S a charging effect occurred for the samples due to their non-conducting character. We calibrate the energy scale by reference to the C1s peak observed on the spectra and which we attributed to the existence of a small contribution of hydrocarbonated species at the surface of the samples. The binding energy of the C1s line maximum was fixed at 285.0 eV. In these conditions the origin of the binding energy scale corresponds to the Fermi level of the sample. The core levels S 2p, Sb 4d, Tl 5d and Tl 4f were recorded with a 0.1 eV step and the valence band with a 0.2 eV step. Let us note that we estimate to about 10% the contribution of carbon contamination. A low contribution of oxygen was observed; it is difficult to estimate its proportion because the O 1s peak is located close to the Sb $3d_{5/2}$ line. Nevertheless its contribution is less than about 5%.

In the case of non-monochromatized incident radiation, the incident beam consists of the main MgK$\alpha_{1,2}$ peak accompanied by satellite lines α_3, α_4 etc. The energy distances between α_3, α_4 (most intense satellites) and the main $\alpha_{1,2}$ doublet are 8.4 eV and 10.0 eV. For samples containing Tl atoms, the Tl $5d_{3/2,\,5/2}$ peak observed around 13–15 eV is accompanied by lower intensity lines due to the excitation of the same core level by the MgKα_3, α_4 satellites, and their contributions are located precisely in the valence band energy range. Consequently a correction to the photoelectron spectra is necessary and has been achieved after a Shirley-type background subtraction, following the current method.

The X-ray emissions S K$\alpha_{1,2}$ ($2p_{3/2,1/2} \rightarrow 1s$) and S K$\beta$ ($3p \rightarrow 1s$) spectra were recorded with a curved crystal X-ray spectrometer [9]. The monochromator was a quartz (1011) crystal ($d = 334.275$ nm) curved under 250 mm and used in the 1st order of reflection. A proportional Ar/CH_4 counter was used as a detector. The total instrumental broadening resulting mainly from the crystal is estimated to 0.2 eV. The spectra were excited with an electron beam (5 kV, 5 mA); no modifications of the spectra were observed during the acquisition. The spectra were scanned with a 0.1 eV (Kα) or 0.2 eV (Kβ) step width. They are obtained as a function of the photon energy (X-ray transition energy), that is E(S 1s) − E(S 3p) for S Kβ. On this energy scale, the Fermi level position corresponds to the core level binding energy E(S 1s). We have determined this binding energy value for each sample in the usual way, combining XPS data for the S $2p_{3/2}$ binding energy and XES determination of the S K$\alpha_{1,2}$ ($2p_{3/2,\,1/2} \rightarrow 1s$) X-ray transition energy. Then E^F(S 1s) = E(S Kα_1) + E(S $2p_{3/2}$).

3. Crystal structures

The structures of Sb_2S_3, Tl_2S, $TlSbS_2$ and $TlSb_3S_5$ are rather complex, and each element of these compounds occupy different crystallographic sites. We give a simple picture of the structures. The environment of Sb can be described by three different units: trigonal pyramids SbS_3, trigonal bipyramids SbS_4 and square pyramids SbS_5. The mean Sb–S bond lengths (2.4–2.6Å) indicate a rather covalent character. Except for Tl_2S the high value of the coordination number of Tl (5–7 atoms) and the Tl–S bond lengths (3–3.3Å) can be related to an ionic character for the Tl–S bonds.

Sb_2S_3 is a ribbon material [10]. The ribbons can be described by $(Sb_4S_6)_n$ units which are formed by two edge-sharing square pyramids SbS_5 connected to two trigonal pyramids SbS_3. There are two sites for Sb: $1xSbS_3 + 1xSbS_5$ and three sites for S: $1xSSb_2 + 2xSSb_3$. The chains interact slightly by the long bonds Sb–S between trigonal pyramids.

Tl_2S is a layer material (anti-CdI_2) [11]. The layers are formed by very distorted octahedra STl_6 connected by the edges. There are six different sites for Tl, which are surrounded by 3 S to form trigonal pyramids TlS_3 and five sites for S which form very distorted octahedra. The layers are slightly connected by Tl–Tl bonds.

$TlSbS_2$ is a layer material [12]. The layers are formed by chains of Sb–S and Tl–S. There are two Sb sites which form SbS_4 trigonal bipyramids, four S sites: $2xSSb_2Tl_2 + 2xSSb_2Tl_2$ and two Tl sites surrounded by 7 S.

$TlSb_3S_5$ is formed by sheets $(Sb_3S_5)_n$ connected by $(TlS_5)_n$ chains to form a three-dimensional network [13]. There are three Sb sites: $2xSbS_3 + 1xSbS_4$, five S sites: $2xSSb_2 + 2xSSb_2Tl + 1xSSb_2Tl_2$ and one Tl site surrounded by 5 S.

4. Results and discussion

4.1. Core levels

The S 2p spectra from Tl_2S, Sb_2S_3, $TlSbS_2$ and $TlSb_3S_5$ are reported as a function of binding energy in Fig. 1. The lines are asymmetric, revealing the spin–orbit splitting $2p_{1/2}$–$2p_{3/2}$. Significant changes appear between the spectra, as the composition of the sample varies. We observe a large shift towards higher binding energy of the maximum intensity of the peak when going from Tl_2S to Sb_2S_3, and a noticeable broadening of the line. The splitting effect which is clearly evidenced for Tl_2S is smoothed out in Sb_2S_3 and in ternary compounds.

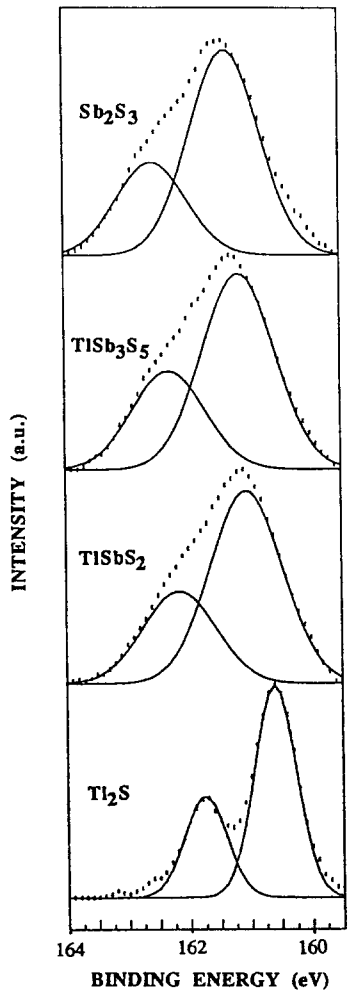

Fig. 1. S $2p_{1/2,3/2}$ core level XPS spectra from Tl_2S, $TlSbS_2$, $TlSb_3S_5$, Tl_2S. Experimental curves (dotted line) are fitted to a sum of two gaussian curves S $2p_{1/2}$, S $2p_{3/2}$ (solid line).

A two gaussian peak reconstruction of the spectra using a least squares fit program has been performed to simulate the spin–orbit splitting of the S 2p line. The assumption are the following: the separation $2p_{1/2}$ and $2p_{3/2}$ is equal to $\Delta E = 1.1 \pm 0.1$ eV [14], the intensity ratio between the lines is 1/2 and their FWHM are identical for a same compound. (This assumes a single type of environment for S atoms.) The mean S $2p_{3/2}$ energy and linewidth obtained from this decomposition procedure are reported in Table 1. On going from Tl_2S to Sb_2S_3, the S $2p_{3/2}$ binding energy (BE) increases by 0.9 eV; the increase in BE is accompanied by a significant increase of the width of the line, from 1.0 to 1.4 eV. For ternary compounds the binding energy values are close to that of Sb_2S_3, but slightly lower; their widths are slightly broader than that of Sb_2S_3.

The binding energy of a core level is sensitive to the chemical environment of the emitting atom. When the chemical bonding is modified, binding energy shifts of the core levels are observed: they are due to modifications of the charge transfer occurring between the emitting atom and its first neighbours. In our case, S atoms are more electronegative than Sb or Tl atoms and a charge transfer occurs from Sb or Tl to S atoms. The electronegativity χ values are 2.5, 1.9 and 1.8 for S, Sb and Tl respectively [15]. The increase of S 2p BE on going from Tl_2S to Sb_2S_3 reveals that the charge transfer to S atoms is higher for Tl–S than for Sb–S, in agreement with the higher $\Delta\chi$ value of the bond in Tl–S than in Sb–S.

The width of S $2p_{3/2}$ is noticeably smaller in Tl_2S than in Sb_2S_3 or in ternary compounds, which reveals that charge fluctuations around S atoms due to different bonding sites or different bond lengths are much lower in Tl_2S than in Sb_2S_3 and ternary compounds.

X-ray absorption measurements at the K edge of S have been performed for the same samples [5]. From these results, the first absorption line corresponding to the $1s \rightarrow 3p$ transition, which gives information on the S environment, is broader and more asymmetric for

Table 1
Binding energies and FWHM of S $2p_{3/2}$, Sb $4d_{5/2}$, Tl $5d_{5/2}$ and Tl $4f_{5/2}$

Compound	S $2P_{3/2}$		Sb $4d_{5/2}$		Tl $5d_{5/2}$		Tl $4f_{7/2}$	
	BE	FWHM	BE	FWHM	BE	FWHM	BE	FWHM
Sb_2S_3	161.4	1.4	33.2	1.4				
$TlSb_2S_5$	161.2	1.5	33.0	1.5_5	12.8	1.6	118.1	1.6
$TlSbS_2$	161.1	1.5	32.9	1.4_5	12.7	1.5	118.1	1.5_5
Tl_2S	160.5	1.0			12.7	1.2	118.1	1.3_5

$TlSbS_2$ than Sb_2S_3. This reveals a more complex atomic bonding for ternary compounds, in agreement with core levels results.

The Sb $4d_{5/2}$, Tl $5d_{5/2}$ and Tl $4f_{7/2}$ core level binding energies are reported in Table 1. Sb $4d_{5/2}$ BE is obtained from a reconstruction of the $4d_{3/2,5/2}$ doublet assuming an intensity ratio of the lines equal to 2/3 and an energy separation of 1.3 eV [14]. The Sb and Tl core level binding energies are less sensitive to changes in local bonding and the energy shifts observed remain within the limits of experimental uncertainty. Similarly, the Sb $4d_{5/2}$ width is barely modified when going from Sb_2S_3 to ternary compounds. On the contrary, the widths of the Tl $5d_{5/2}$ and Tl $4f_{7/2}$ core levels are strongly broadened from Tl_2S to ternary compounds (Table 1). These effects reveal clearly that charge fluctuations around Tl atoms are higher in ternary compounds compared with Tl_2S, in agreement with the results from the S 2p core level.

4.2. Valence band

In Fig. 2 we have reported on a common energy scale the XPS valence band spectra from Tl_2S, Sb_2S_3, $TlSbS_2$ and $TlSb_3S_5$ samples and the S Kβ X-ray spectra from the same samples. The amplitude of the spectra are normalized between their minimum and maximum values.

For compounds containing Tl atoms, the curves have been corrected for the contribution induced by satellite lines MgKα_3,α_4, as indicated in Section 2. The curves are plotted between the Fermi energy (E_F) and 10 eV, the contribution of Tl $5d_{5/2}$ becoming important for higher binding energy. Let us recall that the XPS valence band corresponds to the density of states of the valence band modulated by photo-ionization cross-sections (σ). The valence band of chalcogenides consist of s and p states from Tl, Sb and S. From the σ atomic values calculated by Scofield [16], the p valence states of Sb and S have a higher contribution than Tl p states and p states correspond to higher σ values than p-symmetry states.

S Kβ spectra reflect the S 3p states distributions broadened by the Lorentzian contribution of the S 1s core level of sulphur which is approximately 0.5 eV in pure sulphur [17]. The uncertainty in the adjustment of the binding energy scale of the XPS and XES spectra is about 0.5 eV.

For Tl_2S the valence band consists of three well-resolved peaks located at about 2.0, 4.5 and 7.5 eV. Our VB spectrum is in qualitative agreement with previous results, although the two higher BE structures are not quite well-resolved in Ref. [18]. The overall distribution is similar to that of a covalent semiconductor with three distinct parts, which could be attributed to p, sp and s states as binding energy

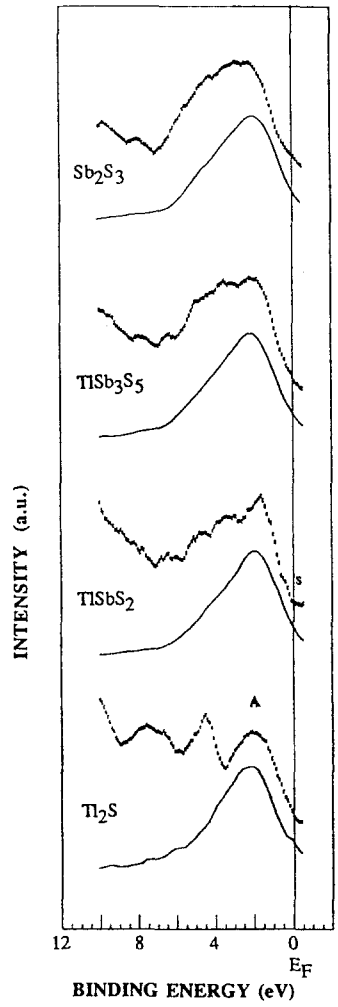

Fig. 2. Valence band XPS spectra (solid line) and S Kb X-ray spectra from Tl_2S, $TlSbS_2$, $TlSb_3S_5$ and Sb_2S_3 adjusted in a common binding energy scale, with E_F as the origin.

increases. From the comparison of XPS and XES data, it seems that S 3p states correspond to the low binding energy region of the XPS valence band curve; the edges of both curves have nearly the same slope.

In Sb_2S_3 the XPS valence band shape is completely changed: it shows a wide rounded peak between E_F and 7.5 eV where a minimum occurs. Beyond this energy, we note an increase of the curve with a small bump at 8.5 eV. The S 3p distribution is located near the top of the valence band; it is more extended towards high binding energy than in Tl_2S and consequently is broader than S 3p from Tl_2S. However, its overall shape is similar to that of Tl_2S. On the XPS valence band curve, a change of slope occurs at about half amplitude, which involves a sort of tail at low binding energy. This tail is not observed on the S 3p curve.

In the ternary systems $TlSbS_2$ and $TlSb_3S_5$ the XPS valence bands have an intermediate shape between those of Tl_2S and Sb_2S_3. For $TlSbS_2$, a low binding

energy peak A is still observed and the following structures are smoothed. It is noteworthy that for this compound the low binding energy edge is steeper than in other compounds and a shoulder labelled S is detected at 0.7 eV BE. For S 3p the low binding energy edge is not structured; beyond the maximum of the curve the slope is not quite uniform.

In $TlSb_3S_5$ the feature A is hardly resolved from the rest of the curve. It corresponds approximately to the maximum of the S 3p distribution and both XPS VB and S 3p curves are broadened compared with the corresponding $TlSbS_2$ curves.

Let us note that the broadening of S 3p and of the VB distributions in Sb_2S_3 and in ternary compounds compared with Tl_2S are consistent with the increase of S 2p width and similarly can be related to higher charge fluctuations around S atoms present in Sb_2S_3 and ternary compounds, compared with Tl_2S.

We note a slight receding of the valence band edge on going from Tl_2S to Sb_2S_3: about 0.5 eV measured at half amplitude of the edge. This would reveal an increase of the optical gap, assuming that the conduction band edge is not shifted. In ternary compounds the binding energy edge is located at an intermediate energy position.

Band structure calculations have been performed for several antimony chalcogenides by Lefebvre et al. [6] in the tight-binding method. These calculations are based on molecular models to represent the complex atomic structure of the compounds. In the case of $TlSbS_2$, we can compare our experimental results with the theoretical curves. From this comparison, it is possible to attribute the non-uniform shape of the high binding energy edge of the S 3p distribution to the separation of the non-bonding–bonding (S–Sb) p-symmetry states of sulphur. The increase of intensity observed in the XPS valence band beyond 7.7 eV can be attributed to the presence of the Sb s states' contribution. The shoulder labelled S on the XPS curve could reveal the existence of a Tl 6s lone pair.

Density of state calculations are being performed for other chalcogenide compounds, and the comparison with our experimental results will be published for several systems of the Tl_2S–Sb_2S_3 series in a separate paper.

References

[1] C.H.L. Goodman, *Mater. Res. Bull., 20* (1985) 237.

[2] J. Olivier-Fourcade, A. Ibanez, J.C. Jumas, M. Maurin, I. Lefebvre, P. Lippens, M. Lannoo and G. Allan, *J. Solid State Chem., 87* (1990) 366.

[3] J. Olivier-Fourcade, P.E. Lippens, J.C. Jumas, M. Womes, I. Lefebvre, M. Lanno, J.M. Esteva and R. Karnatak, *Eur. J. Solid State Inorg. Chem., 30* (1993) 139.

[4] N. Rey, *Thèse Doctorat 3e cycle*, Montpellier, 1988.

[5] J. Olivier-Fourcade, A. Ibanez, J.C. Jumas, H. Dexpert, C. Blancard, J.M. Esteva and R.C. Karnatak, Eur. *J. Solid State Inorg. Chem., 28* (1991) 409.

[6] I. Lefebvre, M. Lannoo, G. Allan, A. Ibanez, J. Olivier-Fourcade, J.C. Jumas and E. Beaurepaire, *Phys. Rev. Lett., 59* (1987) 2471.

[7] I. Lefebvre, M. Lannoo, G. Allan and L. Martinage, *Phys. Rev., B38* (1988) 8593.

[8] J.C. Jumas, J. Olivier-Fourcade, N. Rey and E. Philippot, *Revue de chimie minérale, 22* (1985) 61.

[9] C. Sénémaud, D. Laporte, J.M. André, R. Khérouf, P. Paquier and M. Ringuenet, in R. Benattar (ed.), *Proc. EC02, X-ray Instrumentation*, vol. 1140, 1989, p. 416.

[10] P. Bayjiss and W. Nowacki, *Z. Kristallogr., 135* (1972) 308.

[11] L.I. Man, *Sov. Phys. Cryst., 15* (1970) 3.

[12] N. Rey, J.C. Jumas, J. Olivier-Fourcade and E. Philippot, *Acta Crystallogr., C39* (1983) 971.

[13] M. Gostojic, W. Nowacki and P. Engel, *Z. Kristallogr., 159* (1982) 217.

[14] M. Cardona and L. Ley (eds.), *Photoemission in solid I*, Springer, 1978, p. 265.

[15] L. Pauling, The Nature of the Chemical Bond and the Structure of Molecules and Crystals, Cornell University, New York, 1960.

[16] J.H. Scofield, *J. Electron. Spectrosc., 8* (1976) 129.

[17] M.O. Krause, J.H. Oliver, *J. Phys. Chem. Ref. data, 8* (1979) 329.

[18] L. Porte and A. Tranquard, *J. Sol. Chem., 35* (1980) 59.